

Received June 23, 2020, accepted June 30, 2020, date of publication July 8, 2020, date of current version July 22, 2020.

Digital Object Identifier 10.1109/ACCESS.2020.3007413

Seeding High Brightness Fiber Amplifiers With Multi-Phase Coded Signal Modulation for SBS Effect Management

WENCHANG LAI^{ID}, PENGFEI MA, WEI LIU^{ID}, CAN LI^{ID}, RONGTAO SU^{ID}, YANXING MA, JIAN WU, MAN JIANG, AND PU ZHOU^{ID}

College of Advanced Interdisciplinary Studies, National University of Defense Technology, Changsha 410073, China

Corresponding authors: Pengfei Ma (shandapengfei@126.com) and Pu Zhou (zhoupu203@163.com)

This work was supported in part by the National Natural Science Foundation of China under Grant 61705264 and Grant 61705265, in part by the Hunan Provincial Innovation Construct Project under Grant 2019RS3017, and in part by the Natural Science Foundation of Hunan province, China, under Grant 2019JJ10005.

ABSTRACT We propose a new modulation approach based on multi-phase coded signal (MPCS) to increase stimulated Brillouin scattering (SBS) threshold in high power narrow-linewidth fiber amplifiers. To investigate the SBS suppressing capacity of the proposed modulation technique, the dynamics of SBS process with different spectra are simulated in active fibers with different dopants, core diameters, lengths and pumping lights based on three typical types of pumping sources (976 nm laser diodes, 915 nm laser diodes and 1018 nm fiber lasers). Before simulation, a spectral-correlated combining efficiency criterion based on coherent beam combining (CBC) system is introduced and is set to be identical in different spectra. As a result, compared with the typical white-noise-signal (WNS) and pseudo random bit sequence (PRBS) modulation techniques, the MPCS modulation yields a higher SBS threshold in 915 nm and 1018 nm pumped fiber amplifiers with relatively longer active fiber. Besides, in fiber amplifier constructed by general 20/400 μm active fiber and with 976 nm pumping strategy, MPCS modulation performs better than WNS and PRBS modulation as well. We believe that this modulation signal is expected to be applied in narrow-linewidth, large-mode-area (LMA) high-brightness fiber laser systems to balance the SBS effect and thermal mode instability (TMI) phenomenon.

INDEX TERMS High power narrow-linewidth fiber amplifier, coherent beam combining, stimulated Brillouin scattering, phase modulation.

I. INTRODUCTION

Coherent beam combining (CBC) is a promising technique to break through the brightness limitations of single monolithic fiber amplifier [1]–[8]. As the combining beamlet in CBC system, the power scaling ability of high-brightness, Yb-doped, narrow-linewidth fiber amplifier is one of the significant aspects. Along with the development of output power scaling, the brightness of this type of fiber source is to be restricted by the dual effects of nonlinear stimulated Brillouin scattering (SBS) and thermal-induced mode instability (TMI) [9]–[15]. Specifically, SBS will induce the laser light transferring into the backward Stokes light so that the output

power of the fiber amplifier will be limited and the whole amplification system will be fragile [16]. TMI will cause the dynamical coupling between fundamental mode and higher order modes and consequently impact the beam quality of the fiber amplifier [17].

As for SBS effect, several suppressing techniques have been proposed, such as selecting large mode area, short active fibers [18], [19], applying thermal or stress gradients [20]–[23], acoustic tailoring techniques [24], [25], multi-longitudinal-mode (MLM) fiber oscillator [26], multi-tone injection [27], [28] and phase modulation [29]–[34]. Among all of them, phase modulation technique is a simple and robust approach to mitigate SBS effect and control the linewidth of fiber amplifiers to promise an excellent temporal coherence [35]. Aiming on this approach, some

The associate editor coordinating the review of this manuscript and approving it for publication was Zinan Wang^{ID}.

typical modulation signals have been proposed and applied, which mainly includes sine-wave signal modulation [9], [29], white noise signal modulation [30], [31], pseudo-random bit sequence (PRBS) modulation [10], [32], and piecewise parabolic signal (PPS) modulation [33] and multi-objective nonlinear optimized signal (MONOS) modulation [34]. Within these modulation signals, WNS and PRBS are the two prevail phase modulation techniques in multi-kilowatt level, narrow-linewidth fiber amplifiers [10], [30]–[32].

With the gradual increase of output power, balancing SBS and TMI is becoming more and more important. Previously studies shown that the TMI threshold could be effectively suppressed by gain saturation effect, which could be fulfilled by shifting the pumping wavelength [36]. Compared with the conventional 976 nm pumping manner, adopting 915 nm and tandem pumping strategies are two feasible and promising ways. In fact, a 3.7 kW all fiber narrow linewidth single mode fiber laser pumped by 915 nm laser diode has been demonstrated by simultaneously suppressing nonlinear effects and TMI [14]. In addition, the tandem pumping strategy has also been incorporated into a 4 kW-level narrow-linewidth fiber amplifiers for TMI suppression quite recently [37].

In this manuscript, a new phase modulation signal named multi-phase coded signal modulation (MPCS) is proposed and theoretically analyzed in high power narrow-linewidth fiber amplifiers. MPCS is a periodic, deterministic signal with features that are a function of the modulation frequency and pattern length, which changes the phase of laser at a series of states from 0 to 2π . By introducing a spectral-correlated combining efficiency criteria based on coherent beam combining (CBC) system, the SBS suppressing ability of fiber amplifiers with different modulation techniques are compared in the circumstances of different dopants, core diameters, fiber lengths and pumping manners. Comparing with the typical WNS and PRBS modulation, the overall results show that MPCS modulation has higher SBS threshold in relatively long active fiber with 915 nm and 1018 nm pumping manners, and also has positive SBS suppressing effect in active fiber with core/cladding diameters of $\sim 20/400 \mu\text{m}$ and 976 nm pumping manner.

II. THEORETICAL BACKGROUND

A. THE MATHEMATICAL PRINCIPLE OF MPCS

Multi-phase coded signal is a complicated modulated signal widely used in modern radar and communication systems [38], which can be expressed as

$$s(t) = A \exp[j(2\pi ft + \varphi(t))] \quad (1)$$

where A is the signal amplitude, f is the carrier frequency, $\varphi(t)$ is the phase modulation function over time. In the situation of MPCS, the math function of $\varphi(t)$ can be expressed as:

$$\begin{aligned} \Phi(k) &= (k - 1)^2 / (2^n - 1) - (k - 1), k = 1, \dots, (2^n - 1) \\ \varphi(t) &= B \times \Phi(\text{rem}(\text{fix}(vt) / (2^n - 1)) + 1) \end{aligned} \quad (2)$$

In Equation (2), $\Phi(k)$ is the state function and $2^n - 1$ is the number of MPCS pattern that also means the number of phase

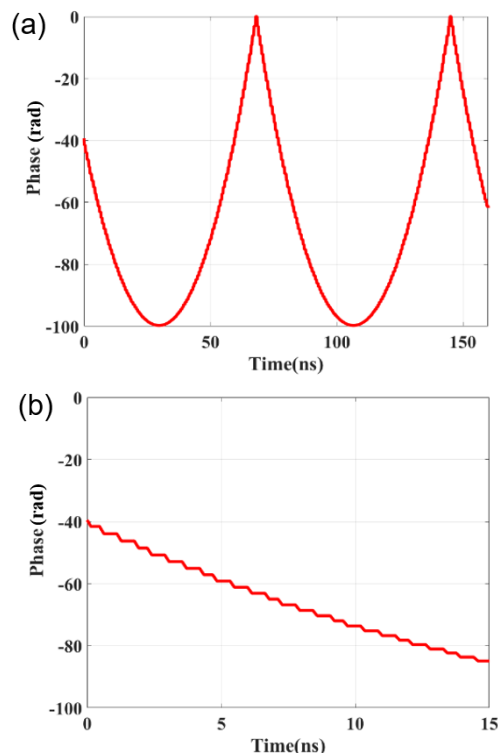


FIGURE 1. (a) The phase of laser modulated by MPCS over a long time range. (b) The phase of laser modulated by MPCS over a short time range.

states in a period. B is the modulated amplitude and ν is the modulated frequency. fix is a rounding function and rem is remainder function.

Here we set that n is equal to 7, which has been proved to be the optimal state for SBS suppression by PRBS modulation [39]. In the following simulation, for fairly compare their capabilities, both the MPCS and PRBS modulations have the same pattern above mentioned. Fig. 1 shows the phase states of laser modulated by MPCS in time domain when modulated amplitude (B) is set to be π and the modulated frequency (ν) is equal to 1.5 GHz. It suggests a nearly periodic parabolic envelope in a long time range as shown in Fig. 1(a). We also show the detail of the phase change in a short time range, which displays a stepped feature in nanosecond (ns) scale as shown in Fig. 1(b). However, the modulated depth shown in Fig. 1 may be too large to realize on experiment. Thus, we can leave the remainder as phase value after the phase $\varphi(t)$ is divided by 2π so that the modulated depth would not exceed 2π , which is more feasible in realization. The SBS suppression effect of MPCS after dividing is proved to be feasible in the following simulation.

The phase after dividing is shown in Fig. 2(a). A series of phase states from 0 to approximately 2π could be generated by MPCS. In addition, MPCS modulation generates a nearly sinc² spectrum as shown in Fig. 2(b). The envelope shown in Fig. 2(b) is similar to the generated optical spectral distribution by PRBS while its degree of denseness is higher. In contrast to WNS, the spectrum created by MPCS

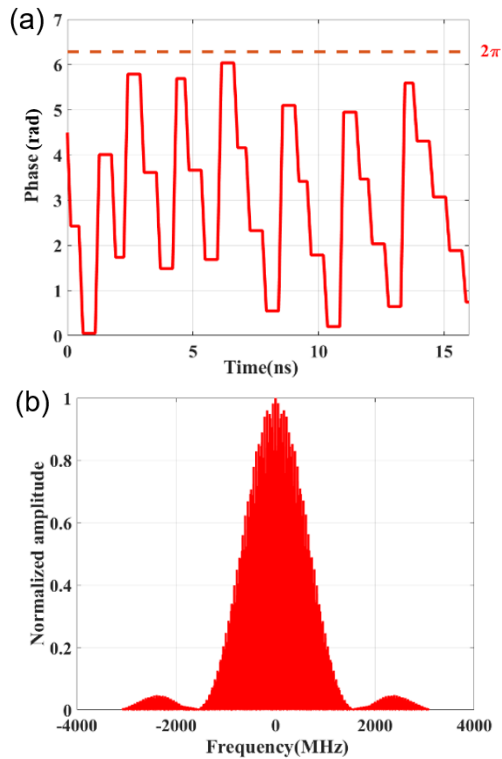


FIGURE 2. (a) The phase of laser modulated by MPCS after dividing over a short time range. (b) The spectrum of laser modulated by MPCS.

shows features such as discreteness and deterministic [34]. For a given modulated frequency (ν_c), each phase state has a duration time of $1/\nu_c$. The sinc² spectrum has nulls located at integer multiples of ν_c and $-\nu_c$. The pattern length controls the number of discrete spectral components within that envelope. The line spacing can be calculated by $\nu_c/2^n - 1$.

B. THE THEORETICAL MODEL OF SBS EFFECT

In this section, we introduce a detailed model to analyze the SBS process in active fiber amplifier. In the theoretical analysis of SBS in optical fibers, transient coupled wave equations describe the evolution of the laser field, the Stokes field and the phonon field correctly [39]. Here we further consider the active amplifying effect occurring in the amplifier. And the self-phase modulation and cross-phase modulation between the signal light and the Stokes light are also taken into consideration. The normalized amplitudes of the laser light (A_S), the Stokes light (A_B), and the phonon field (Q) satisfy the following equations [40].

$$\frac{\partial A_S}{\partial z} + \frac{1}{v_{gs}} \frac{\partial A_S}{\partial t} = -\frac{\alpha_S}{2} A_S + \frac{1}{2} [(\sigma_{as} + \sigma_{es}) N_2 - \sigma_{as} N] A_S + i\gamma_S (|A_S|^2 + 2|A_B|^2) A_S + i\kappa_{1s} A_B Q \quad (3)$$

$$-\frac{\partial A_B}{\partial z} + \frac{1}{v_{gB}} \frac{\partial A_B}{\partial t} = -\frac{\alpha_B}{2} A_B + \frac{1}{2} [(\sigma_{as} + \sigma_{es}) N_2 - \sigma_{as} N] A_B + i\gamma_S (|A_B|^2 + 2|A_S|^2) A_B + i\kappa_{1B} A_S Q^* \quad (4)$$

$$\frac{\partial Q}{\partial t} + v_A \frac{\partial Q}{\partial z} = -\left[\frac{1}{2} \Gamma_B + i(\Omega_B - \Omega)\right] Q + i \frac{\kappa_2}{A_{ao}} A_S A_B^* + f \quad (5)$$

where v_{gs} and v_{gB} are the group speed of signal laser and Stokes light, v_A is the acoustic velocity in active fiber. α_S and α_B are the attenuation of signal laser and Stokes light in active fiber. σ_{as} and σ_{es} are the absorption cross-section and emission cross-section of signal laser. γ_S is the non-linear coefficient of signal laser and Γ_B is the acoustic damping ratio. Ω_B represents the acoustic angular frequency while the Ω indicates the varied angular frequency. κ_{1S} , κ_{1B} and κ_2 are coupling coefficients of the signal laser, Stokes, and acoustic fields, respectively. A_{ao} is the effective interaction area of the light field and the acoustic field. f is the heat noise that arises the SBS spontaneously, which can be expressed as [41]

$$\langle f(z, t) f^*(z', t') \rangle = N_Q \delta(z - z') \delta(t - t') \quad (6)$$

$$N_Q = \frac{2kT_0 \rho_0 \Gamma_B}{v_A^2 A_{eff}} \quad (7)$$

$$\langle f(z, t) \rangle = 0 \quad (8)$$

where k is Boltzmann Constant and ρ_0 is the density of fiber, T_0 is the temperature and A_{eff} is the effective mode area that is equal to the fiber core area in this simulation. Except for the laser, Stokes and phonon fields, the pumping light of amplifier, which has the same propagation direction of signal laser in this model, could be calculated by laser rate equation as shown below.

$$\frac{\partial P_p}{\partial z} + \frac{1}{v_{gp}} \frac{\partial P_p}{\partial t} = -\alpha_p P_p - \Gamma_p [\sigma_{ap} N - (\sigma_{ap} + \sigma_{ep}) N_2] P_p \quad (9)$$

In (9), P_p means the pump power. v_{gp} is the group speed of pump light in active fiber. α_p is the absorption coefficient of pump light in fiber. σ_{ap} and σ_{ep} are absorption cross-section and emission cross-section of pump light in active fiber. N and N_2 represent the number of doped Yb⁺ particles and excited Yb⁺ particles at upper-energy state. In fact, N_2 obey the following equation.

$$\frac{\partial N_2}{\partial t} = -\frac{N_2}{\tau} + \frac{\Gamma_s \lambda_s}{hc A_c} [\sigma_{as} N - (\sigma_{as} + \sigma_{es}) N_2] (P_s + P_B) + \frac{\Gamma_p \lambda_p}{hc A_c} [\sigma_{ap} N - (\sigma_{ap} + \sigma_{ep}) N_2] P_p \quad (10)$$

where τ is the average lifetime of Yb⁺ at upper-energy state. c is the speed of light in vacuum, h is Planck Constant and A_c is the doped area. Γ_s and Γ_p are the overlapping factors of signal light and pump light, respectively. P_s , P_B and P_p represent the signal power, Stokes power and pump power respectively.

In the simulations, a typical parallelizable, bidirectional (PB) numerical algorithm is employed [42] and the typical and universal parameters of active fiber are present in Table 1.

TABLE 1. Parameters used in model.

Symbol	Quantity	Value
λ_s	Signal laser wavelength	1064.0 nm
λ_B	Stokes light wavelength	1064.1 nm
n_{co}	Refractive index of signal laser (Stokes light)	1.451
n_p	Refractive index of pump light	1.415
A_{ao}	Interaction area between light and sound	$2.6543 \times 10^{-10} \text{ m}^2$
τ	Yb ⁺ lifetime	840 μs
γ_s	Nonlinear coefficient of signal laser	0.902
Γ_B	Acoustic damping rate	2.0552×10^8
Γ_P	Overlap factor of pump light	0.0025
Γ_S	Overlap factor of signal laser	1.0000
α_p	Attenuation of pump	2.1 dB/km
α_s	Attenuation of signal	15 dB/km
T_0	Temperature	293 K
ρ_0	Fiber density	2210.0 kg/m ³
v_A	Velocity of sound	5897.4 m/s
N	Doping concentration of Yb ⁺	$7.8189 \times 10^{25} / \text{m}^3$
Ω_B	Acoustic angular frequency	$1.0106 \times 10^{11} \text{ rad}$

C. A SPECTRAL-CORRELATED COMBINING EFFICIENCY CRITERION

Before simulation, a criterion that could be employed to compare the SBS suppression effect of different modulated signals and explore the advantages of MPCS modulation technique is strongly required. One conventional route seems to be feasible is to compare the SBS threshold at identical ‘‘spectral linewidth’’. In previous studies, different definitions of ‘‘spectral linewidth’’ of narrow-linewidth fiber amplifier, such as full-width at half-maximum (FWHM) [31], 85% fraction of total power [33] and root-mean-square (RMS) [34], have been proposed. However, different spectral distributions or spectral envelopes could be produced by using different modulation signals. The multiplicity of definition of spectral linewidth would bring inconvenience in comparing the SBS suppressing ability of spectra with different envelopes. In order to overcome the difficulties above, we directly employ the relationship between combining efficiency of CBC system and the spectral distribution, and compare the SBS thresholds of different modulation signals under identical combining efficiency. By doing this, the ununiformed definitions of ‘‘spectral linewidth’’ could be avoided. Without loss of generality, based on a typical two-channel coaxially CBC system with delay time of τ , the spectral-correlated combining efficiency could be expressed by [43]

$$\eta = \frac{1}{2} + \frac{\sum_{n=1}^N P_n \cos(2\pi \nu_n \tau)}{2 \sum_{n=1}^N P_n} \quad (11)$$

where ν_n is the frequency of spectrum and N is the total number of spectral lines in spectrum. P_n is the power intensity at frequency of ν_n in spectrum. From the theoretical analysis

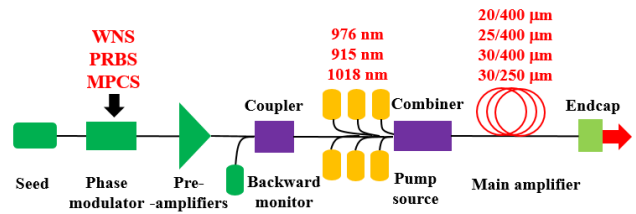


FIGURE 3. Schematic of MOPA structure in the simulation.

above, a spectral-correlated combining efficiency criterion is introduced and can be determined by the distribution of spectrum, which is suitable for arbitrary spectra. Thus, under the same combining efficiency, the SBS suppressing capabilities of different modulation signals could be compared by calculating and comparing their SBS thresholds.

III. RESULTS

In this section, we show the SBS suppression effect in three different pumping manners, namely 976 nm laser diodes, 915 nm laser diodes and 1018 nm fiber lasers for tandem pumping. As depicted above, even pumped by 976 nm laser diodes is prefer for SBS suppression due to its highly efficient absorption in Yb-doped fiber amplifier, the 915 nm and 1018 nm pumping manners have high TMI thresholds. Thus, the analysis is especially focused on high power, narrow-linewidth fiber amplifiers by simultaneously balancing SBS and TMI.

In the following simulations, without loss of generality, the delay time τ is set to be 0.16 ns, which corresponds with a typical optical path difference nearly 5 cm in the CBC system [44]. The coherent combining efficiency of each spectrum is made to be equal to 87.5% by applying suitable modulated depth and frequency. In this circumstance, the typical FWHMs of spectra modulated by WNS, PRBS and MPCS are calculated to be about 1 GHz, 1.5 GHz, and 1.5 GHz, respectively. The injected seed power is set to be 18 W and the total absorption coefficient is set to be about 13.5 dB to ensuring sufficient pump absorptions at each pumping wavelength. Besides, in each situation, considering the practical application, 3 m delivery passive fiber is followed behind the active fiber. The typical schematic in our simulation is shown in Fig. 3, which is based on the MOPA structure. A modulated seed laser is pre-amplified firstly and then injected into the main amplifier, between which a coupler is used to monitor the backward Stokes power. As described above, the ratio of backward Stokes power to output power (defined as ‘‘reflectivity’’) would increase nonlinearly when SBS threshold appears. Thus, we consider the output power as the SBS threshold when the reflectivity gets to be 0.02% and increases dramatically with the laser output power.

Firstly, the SBS suppressing effects of different modulation signals (MPCS, WNS, PRBS) are calculated based on 976 nm pumping manner. In this case, the cladding absorption coefficients are set to be 1.5 dB/m in 20/400 μm active fiber, 2.4 dB/m in 25/400 μm active fiber and 2.7 dB/m

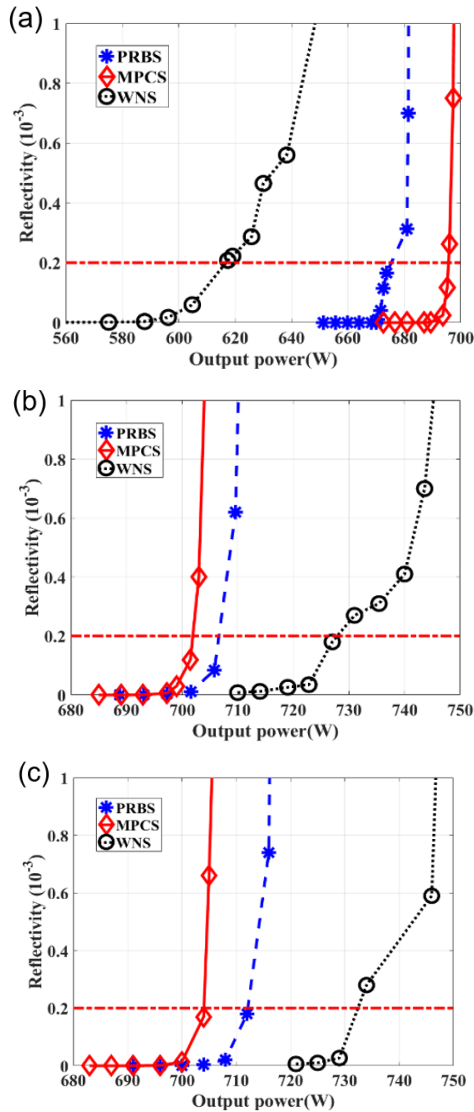


FIGURE 4. Reflectivity vs. the output power in different fiber amplifiers pumped by 976 nm light (a) 20/400 μm fiber with 9 m, (b) 25/400 μm fiber with 5.625 m, (c) 30/400 μm fiber with 5 m.

in 30/400 μm active fiber, respectively. The corresponding fiber lengths are about 9 m, 5.625 m and 5 m, respectively. As for different types of active fiber, the increase trend of reflectivity along with the output power is shown in Figs. 4(a)-(c).

The threshold is marked with a red dotted line where the reflectivity reaches to 0.02% and increases dramatically. As for 20/400 μm active fiber, the calculated SBS threshold of MPCS is ~ 690 W, which is 1.11 times and 1.03 times higher than the WNS and PRBS modulations, respectively. However, for 25/400 μm active fiber, the SBS threshold of MPCS is ~ 702 W, which is 1.04 times lower than the WNS modulations and is almost the same with PRBS modulation. For 30/400 μm active fiber, the situation is similar to that in 25/400 μm active fiber. Based on the analysis above, it could be concluded that the MPCS has a more positive effect on

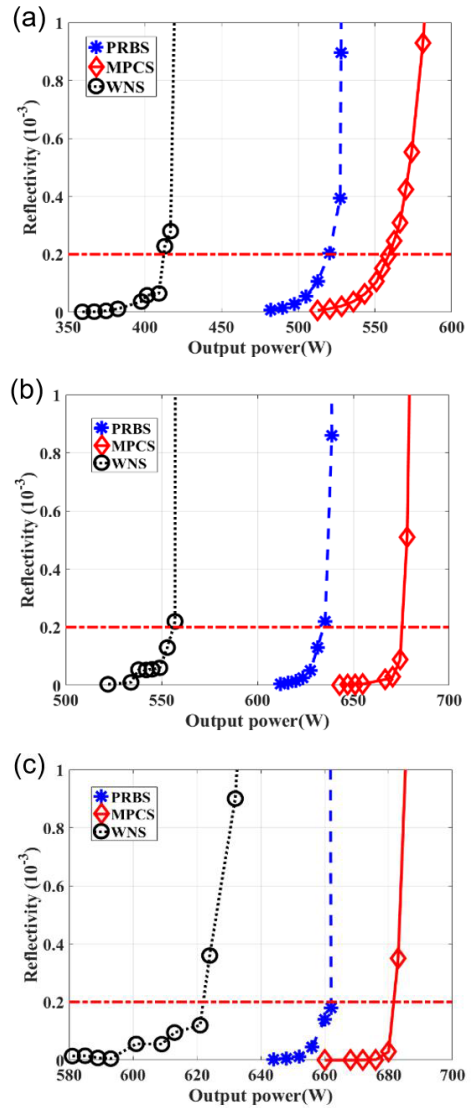


FIGURE 5. Reflectivity vs. the output power in different fiber amplifiers pumped by 915 nm light (a) 20/400 μm fiber with 24.5 m, (b) 25/400 μm fiber with 16.875 m, (c) 30/400 μm fiber with 13.5 m.

SBS suppressing than PRBS and WNS by using 20/400 μm active fiber for constructing fiber amplifiers. Besides, due to the TMI threshold will increase with the decrease of active fiber core size, compared with 25/400 μm and 30/400 μm active fibers, the 20/400 μm active fiber has higher TMI threshold in a practical narrow-linewidth fiber system [36].

Then, we analyze the situation that the pumping light operates at 915 nm. In reality, the absorption coefficient in 915 nm pumped fiber amplifier is much lower than that in fiber amplifier pumped by 976 nm light. In our simulations, they are set to be 0.55 dB/m in 20/400 μm fiber, 0.8 dB/m in 25/400 μm fiber and 1 dB/m in 30/400 μm fiber. The corresponding fiber lengths are calculated to be 24.5 m, 16.875 m and 13.5 m respectively, which promises a total pump absorption of ~ 13.5 dB at 915 nm. Fig. 5 shows the results in the three different fiber amplifiers pumped by 915 nm laser diodes.

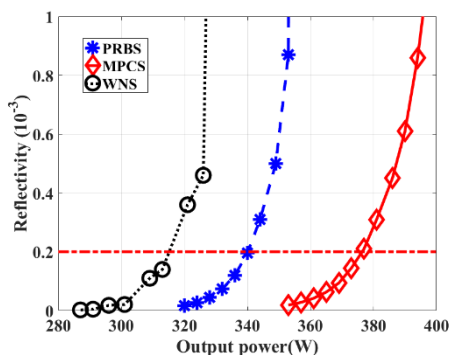


FIGURE 6. Reflectivity vs. the output power in tandem pumping 30/250 μm fiber amplifier with 40 m.

The MPCS modulation presents a significant superiority on SBS threshold improving in all the fiber amplifiers here. In the 20/400 μm fiber with a length of 24.5 m, the SBS threshold we obtained by MPCS modulation is about 560 W, exceeding 40 W than that modulated by PRBS and being 1.3 times than that modulated by WNS. The advantage also exists in 25/400 μm fiber with a length of 16.875 m. The MPCS modulation improves the SBS threshold by 10% compared with PRBS modulation and 20% compared with WNS modulation. When the core diameter is increased to 30 μm , MPCS still has highest SBS threshold of 680 W while the other two modulation techniques has threshold of 660 W (PRBS) and 620 W (WNS) respectively. It is no doubt here that MPCS modulation are more suitable to be applied in fiber amplifier pumped by 915 nm laser diodes.

In the last section, the process of SBS in fiber amplifier adopting tandem pumping technique with 1080 nm fiber laser is simulated. Because that the cladding absorption coefficient at 1018 nm in Yb-doped active fiber is small, highly doped, large-mode-area active fiber should be adopted for favorable of stimulated Raman scattering (SRS) effect. In the previous experiment, normally active fiber with core diameter of 30 μm and inner cladding diameter of 250 μm is employed [45]. In the simulation, the pumping absorption coefficient at 1018 nm is set to be 0.34 dB/m and as long as 40 m active fiber is adopted.

The simulating results are present in Fig. 6. It is obvious that MPCS modulation also presents best performance in tandem pumping fiber amplifier compared with WNS and PRBS. It has a SBS threshold of 380W which exceeding more than 10% and 20% than those modulated by PRBS and WNS respectively. As we all know, tandem pumping has very little quantum defect so that it can produce little heat and has a high TMI threshold. We believe that the MPCS modulation technique we proposed could play a key role on balancing the SBS and TMI to achieve higher power output in tandem pumping fiber laser system.

IV. CONCLUSION

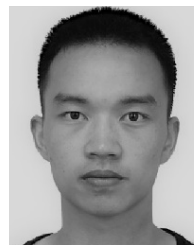
In summary, we have presented MPCS phase modulation for SBS management in high power narrow linewidth fiber amplifier for the firstly time to the best of our

knowledge. It provides determined multi-phase states varying from 0 to 2π and generates a discrete nearly sinc² optical spectrum. To explore its application on balancing SBS and TMI, a theoretical model is introduced to calculate the amplifying process in fiber amplifier pumped by 976 nm, 915 nm and 1018 nm (tandem pump) light. Moreover, the advantages on SBS suppressing of MPCS with that of WNS and PRBS techniques are compared with a standard based on coherent combining efficiency. We find that MPCS modulation presents better performance on improving SBS threshold in the case of 915 nm pumping and tandem pumping. Besides, in a general 20/400 μm fiber amplifier pumped by 976 nm laser diodes, MPCS also shows better SBS suppressing capacity compared with WNS and PRBS. Overall, MPCS modulation has great potential on balancing SBS and TMI effect in fiber amplifier and achieving higher power laser output at narrow linewidth, which could have significant impact on high power beam combining system.

REFERENCES

- [1] T. Y. Fan, "Laser beam combining for high-power, high-radiance sources," *IEEE J. Sel. Topics Quantum Electron.*, vol. 11, no. 3, pp. 567–577, May 2005.
- [2] L. Siiman, W.-Z. Chang, T. Zhou, and A. Galvanauskas, "Coherent femtosecond pulse combining of multiple parallel chirped pulse fiber amplifiers," *Opt. Express*, vol. 20, no. 16, pp. 18097–18116, Jul. 2012.
- [3] H. K. Ahn and H. J. Kong, "Cascaded multi-dithering theory for coherent beam combining of multiplexed beam elements," *Opt. Express*, vol. 23, no. 9, pp. 12407–12413, May 2015.
- [4] A. Flores, I. Dajani, R. Holten, T. Ehrenreich, and B. Anderson, "Multi-kilowatt diffractive coherent combining of pseudorandom-modulated fiber amplifiers," *Opt. Eng.*, vol. 55, no. 9, Sep. 2016, Art. no. 096101.
- [5] Z. Liu, P. Ma, R. Su, R. Tao, Y. Ma, X. Wang, and P. Zhou, "High-power coherent beam polarization combination of fiber lasers: Progress and prospect [invited]," *J. Opt. Soc. Amer. B, Opt. Phys.*, vol. 34, no. 3, p. A7, Mar. 2017.
- [6] C. Peng, X. Liang, R. Liu, W. Li, and R. Li, "High-precision active synchronization control of high-power, tiled-aperture coherent beam combining," *Opt. Lett.*, vol. 42, no. 19, pp. 3960–3963, Oct. 2017.
- [7] D. Kabeya, V. Kermène, M. Fabert, J. Benoist, J. Saucourt, A. Desfarges-Berthelemot, and A. Barthélémy, "Efficient phase-locking of 37 fiber amplifiers by phase-intensity mapping in an optimization loop," *Opt Express*, vol. 25, no. 12, pp. 13816–13821, Jun. 2017.
- [8] M. Muller, A. Klenke, A. Steinkopf, H. Stark, A. Tunnermann, and J. Limpert, "3.5 kW coherently combined ultrafast fiber laser," *Opt. Lett.*, vol. 43, no. 24, pp. 6037–6040, Dec. 2018.
- [9] P. Ma, R. Tao, R. Su, X. Wang, P. Zhou, and Z. Liu, "1.89 kW all-fiberized and polarization-maintained amplifiers with narrow linewidth and near-diffraction-limited beam quality," *Opt. Express*, vol. 24, no. 4, pp. 4187–4195, Feb. 2016.
- [10] M. Liu, Y. Yang, H. Shen, J. Zhang, X. Zou, H. Wang, L. Yuan, Y. You, G. Bai, B. He, and J. Zhou, "1.27 kW, 2.2 GHz pseudo-random binary sequence phase modulated fiber amplifier with Brillouin gain-spectrum overlap," *Sci. Rep.*, vol. 10, no. 1, pp. 1–8, Jan. 2020.
- [11] J. O. White, M. Harfouche, J. Edgecumbe, N. Satyan, G. Rakuljic, V. Jayaraman, C. Burgner, and A. Yariv, "16 kW yb fiber amplifier using chirped seed amplification for stimulated Brillouin scattering suppression," *Appl. Opt.*, vol. 56, no. 3, p. B116, Jan. 2017.
- [12] B. M. Anderson, A. Flores, and I. Dajani, "Filtered pseudo random modulated fiber amplifier with enhanced coherence and nonlinear suppression," *Opt Express*, vol. 25, no. 14, pp. 17671–17682, Jul. 2017.
- [13] F. Beier, C. Hupel, S. Kuhn, S. Hein, J. Nold, F. Proske, B. Sattler, A. Liem, C. Jauregui, J. Limpert, N. Haarlammert, T. Schreiber, R. Eberhardt, and A. Tunnermann, "Single mode 4.3 kW output power from a diode-pumped Yb-doped fiber amplifier," *Opt. Express*, vol. 25, no. 13, pp. 14892–14899, Jun. 2017.

- [14] H. Lin, R. Tao, C. Li, B. Wang, C. Guo, Q. Shu, P. Zhao, L. Xu, J. Wang, F. Jing, and Q. Chu, "3.7 kW monolithic narrow linewidth single mode fiber laser through simultaneously suppressing nonlinear effects and mode instability," *Opt Express*, vol. 27, no. 7, pp. 9716–9724, Apr. 2019.
- [15] Y. S. Chen, H. Z. Xu, Y. B. Xing, L. Liao, Y. B. Wang, F. F. Zhang, X. L. He, H. Q. Li, J. G. Peng, L. Y. Yang, N. L. Dai, and J. Y. Li, "Impact of gamma-ray radiation-induced photodarkening on mode instability degradation of an ytterbium-doped fiber amplifier," *Opt Express*, vol. 26, no. 16, pp. 20430–20441, Aug. 2018.
- [16] R. G. Smith, "Optical power handling capacity of low loss optical fibers as determined by stimulated Raman and Brillouin scattering," *Appl. Opt.*, vol. 11, no. 11, pp. 2489–2494, Nov. 1972.
- [17] T. Eidam, C. Wirth, C. Jauregui, F. Stutzki, F. Jansen, H.-J. Otto, O. Schmidt, T. Schreiber, J. Limpert, and A. Tünnermann, "Experimental observations of the threshold-like onset of mode instabilities in high power fiber amplifiers," *Opt. Express*, vol. 19, no. 14, pp. 13218–13224, Jun. 2011.
- [18] P. Ma, P. Zhou, Y. Ma, R. Su, X. Xu, and Z. Liu, "Single-frequency 332 W, linearly polarized Yb-doped all-fiber amplifier with near diffraction-limited beam quality," *Appl. Opt.*, vol. 52, no. 20, pp. 4854–4857, Jul. 2013.
- [19] Y. Jeong, J. Nilsson, J. K. Sahu, D. B. S. Soh, C. Alegria, P. Dupriez, C. A. Codemard, D. N. Payne, R. Horley, L. M. B. Hickey, L. Wanzcyk, C. E. Chryssou, J. A. Alvarez-Chavez, and P. W. Turner, "Single-frequency, single-mode, plane-polarized ytterbium-doped fiber master oscillator power amplifier source with 264 W of output power," *Opt Lett*, vol. 30, no. 5, pp. 459–461, Mar. 2005.
- [20] L. Zhang, S. Cui, C. Liu, J. Zhou, and Y. Feng, "170 W, single-frequency, single-mode, linearly-polarized, Yb-doped all-fiber amplifier," *Opt Express*, vol. 21, no. 5, pp. 5456–5462, Feb. 2013.
- [21] L. Huang, H. Wu, R. Li, L. Li, P. Ma, X. Wang, J. Leng, and P. Zhou, "414 W near-diffraction-limited all-fiberized single-frequency polarization-maintained fiber amplifier," *Opt Lett*, vol. 42, no. 1, pp. 1–4, Jan. 2017.
- [22] J. Hansryd, F. Dross, M. Westlund, P. A. Andrekson, and S. N. Knudsen, "Increase of the SBS threshold in a short highly nonlinear fiber by applying a temperature distribution," *J. Lightw. Technol.*, vol. 19, no. 11, pp. 1691–1697, Nov. 2001.
- [23] T. Theeg, H. Sayinc, J. Neumann, and D. Kracht, "All-fiber counter-propagation pumped single frequency amplifier stage with 300-W output power," *IEEE Photon. Technol. Lett.*, vol. 24, no. 20, pp. 1864–1867, Oct. 15, 2012.
- [24] C. Robin, I. Dajani, and B. Pulford, "Modal instability-suppressing, single-frequency photonic crystal fiber amplifier with 811 W output power," *Opt. Lett.*, vol. 39, no. 3, pp. 666–669, Feb. 2014.
- [25] S. Gray, A. Liu, D. T. Walton, J. Wang, M. Li, X. Chen, A. B. Ruffin, J. A. Demeritt, and L. A. Zenteno, "502 Watt, single transverse mode, narrow linewidth, bidirectionally pumped Yb-doped fiber amplifier," *Opt Express*, vol. 15, no. 25, pp. 17044–17050, Dec. 2007.
- [26] M. Jiang, P. Ma, L. Huang, J. Xu, P. Zhou, and X. Gu, "KW-level, narrow-linewidth linearly polarized fiber laser with excellent beam quality through compact one-stage amplification scheme," *High Power Laser Sci. Eng.*, vol. 5, pp. 1–5, Oct. 2017, Art. no. e30.
- [27] P. WeBels, P. Adel, M. Auerbach, D. Wandt, and C. Fallnich, "Novel suppression scheme for Brillouin scattering," *Opt Express*, vol. 12, no. 19, pp. 4443–4448, Sep. 2004.
- [28] I. Dajani, C. Zeringue, and T. M. Shay, "Investigation of nonlinear effects in multitone-driven narrow-linewidth high-power amplifiers," *IEEE J. Sel. Topics Quantum Electron.*, vol. 15, no. 2, pp. 406–414, Apr. 2009.
- [29] D. Engin, W. Lu, M. Akbulut, B. McIntosh, H. Verdun, and S. Gupta, "1 kW cw Yb-fiber-amplifier with <0.5GHz linewidth and near-diffraction limited beam-quality for coherent combining application," *Proc. SPIE*, vol. 7914, Feb. 2011, Art. no. 791407.
- [30] V. R. Supradeepa, "Stimulated Brillouin scattering thresholds in optical fibers for lasers linewidth broadened with noise," *Opt. Express*, vol. 21, no. 4, pp. 4677–4687, Feb. 2013.
- [31] T. Li, C. Zha, Y. Sun, Y. Ma, W. Ke, and W. Peng, "3.5 kW bidirectionally pumped narrow-linewidth fiber amplifier seeded by white-noise-source phase-modulated laser," *Laser Phys.*, vol. 28, no. 10, Jul. 2018, Art. no. 105101.
- [32] A. Flores, C. Robin, A. Lanari, and I. Dajani, "Pseudo-random binary sequence phase modulation for narrow linewidth, kilowatt, monolithic fiber amplifiers," *Opt. Express*, vol. 22, no. 15, pp. 17735–17744, Jul. 2014.
- [33] J. O. White, J. T. Young, C. Wei, J. Hu, and C. R. Menyuk, "Seeding fiber amplifiers with piecewise parabolic phase modulation for high SBS thresholds and compact spectra," *Opt Express*, vol. 27, no. 3, pp. 2962–2974, Feb. 2019.
- [34] A. V. Harish and J. Nilsson, "Optimization of phase modulation formats for suppression of stimulated Brillouin scattering in optical fibers," *IEEE J. Sel. Topics Quantum Electron.*, vol. 24, no. 3, pp. 1–10, May 2018.
- [35] B. Anderson, A. Flores, R. Holten, and I. Dajani, "Comparison of phase modulation schemes for coherently combined fiber amplifiers," *Opt Express*, vol. 23, no. 21, pp. 27046–27060, Oct. 2015.
- [36] R. Tao, X. Wang, and P. Zhou, "Comprehensive theoretical study of mode instability in high-power fiber lasers by employing a universal model and its implications," *IEEE J. Sel. Topics Quantum Electron.*, vol. 24, no. 3, pp. 1–19, May 2018.
- [37] P. Ma, H. Xiao, D. Meng, W. Liu, R. Tao, J. Leng, Y. Ma, R. Su, P. Zhou, and Z. Liu, "High power all-fiberized and narrow-bandwidth MOPA system by tandem pumping strategy for thermally induced mode instability suppression," *High Power Laser Sci. Eng.*, vol. 6, pp. 1–7, Sep. 2018, Art. no. e57.
- [38] N. Levanon, "Multifrequency complementary phase-coded radar signal," *IEEE Proc.-Radar, Sonar Navigat.*, vol. 147, no. 6, pp. 276–284, Dec. 2000.
- [39] C. Zeringue, I. Dajani, S. Naderi, G. T. Moore, and C. Robin, "A theoretical study of transient stimulated Brillouin scattering in optical fibers seeded with phase-modulated light," *Opt. Express*, vol. 20, no. 19, pp. 21196–21213, Sep. 2012.
- [40] Y. Ran, R. Tao, P. Ma, X. Wang, R. Su, P. Zhou, and L. Si, "560 W all fiber and polarization-maintaining amplifier with narrow linewidth and near-diffraction-limited beam quality," *Appl. Opt.*, vol. 54, no. 24, pp. 7258–7263, Aug. 2015.
- [41] R. W. Boyd, K. Rzaewski, and P. Narum, "Noise initiation of stimulated Brillouin scattering," *Phys. Rev. A, Gen. Phys.*, vol. 42, no. 9, pp. 5514–5521, Nov. 1990.
- [42] D. Hollenbeck and C. D. Cantrell, "Parallelizable, bidirectional method for simulating optical-signal propagation," *J. Lightw. Technol.*, vol. 27, no. 12, pp. 2140–2149, Jun. 15, 2009.
- [43] P. Ma, X. Wang, Y. Ma, P. Zhou, and Z. Liu, "Analysis of multi-wavelength active coherent polarization beam combining system," *Opt Express*, vol. 22, no. 13, pp. 16538–16551, Jun. 2014.
- [44] M. A. Vorontsov and T. Weyrauch, "High-power lasers for directed-energy applications: Comment," *Appl. Opt.*, vol. 55, no. 35, pp. 9950–9953, Dec. 2016.
- [45] P. Zhou, H. Xiao, J. Leng, J. Xu, Z. Chen, H. Zhang, and Z. Liu, "High-power fiber lasers based on tandem pumping," *J. Opt. Soc. Amer. B, Opt. Phys.*, vol. 34, no. 3, p. A29, Mar. 2017.



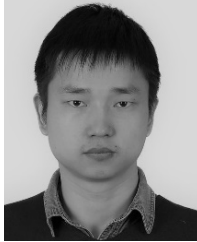
WENCHANG LAI received the B.S. degree in optical engineering from the National University of Defense Technology, Changsha, China, in 2018, where he is currently pursuing the M.S. degree with the College of Advanced Interdisciplinary Studies.



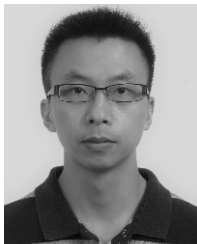
PENGFEI MA received the B.S. degree in optical engineering from Shandong University, Jinan, China, in 2010, and the Ph.D. degree in optical engineering from the National University of Defense Technology, Changsha, China, in 2016. His current research interests include high-power fiber laser technology and coherent beam combination.



WEI LIU received the B.S. and Ph.D. degrees in optical engineering from the National University of Defense Technology, Changsha, China, in 2013 and 2018, respectively. His current research interests include high-power fiber laser/amplifier technology and coherent beam combination.



CAN LI received the Ph.D. degree in engineering from the South China University of Technology, in 2015. From 2015 to 2019, he was a Postdoctoral Fellow with The University of Hong Kong, where he was engaged in developing new technology on fiber lasers and their applications. His current research interests include high-power fiber lasers in the pulsed and continuous-wave regime in the near-/SW-infrared region.



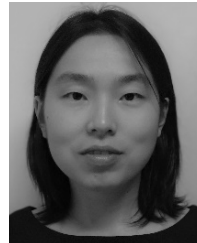
RONGTAO SU received the B.S. and Ph.D. degrees in optical engineering from the National University of Defense Technology, Changsha, China, in 2008 and 2014, respectively. His current research interests include fiber laser/amplifier technology and coherent beam combination.



YANXING MA received the B.S. degree in optical engineering from Shanxi University, Taiyuan, China, in 2006, and the Ph.D. degree in optical engineering from the National University of Defense Technology, Changsha, China, in 2012. His current research interests include fiber laser technology and coherent beam combination.



JIAN WU received the B.S. degree in physics from Central China Normal University, Wuhan, China, in 2006, and the Ph.D. degree in optics from Shanghai Jiao Tong University, Shanghai, China, in 2015. He is currently an Associate Professor with the College of Advanced Interdisciplinary Studies, National University of Defense Technology, Changsha, China. His current research interests include fiber laser technology, analytical chemistry, and plasma physics.



MAN JIANG received the B.S. and Ph.D. degrees in optical engineering from the National University of Defense Technology, Changsha, China, in 2012 and 2017, respectively. Her current research interests include fiber laser technology and beam combining.



PU ZHOU received the B.S. and Ph.D. degrees in optical engineering from the National University of Defense Technology, Changsha, China, in 2005 and 2009, respectively. He is currently a Professor with the College of Advanced Interdisciplinary Studies, National University of Defense Technology. His current research interests include fiber laser/amplifier technology, coherent combining of fiber lasers/amplifiers, and adaptive optics.

...